FEBS Letters 588 (2014) 594–599

FEBS Letters

journal homepage: www.FEBSLetters.org

Identification of an arylalkylamine *N*-acyltransferase from *Drosophila melanogaster* that catalyzes the formation of long-chain *N*-acylserotonins

Daniel R. Dempsey [1], Kristen A. Jeffries [1], Ryan L. Anderson, Anne-Marie Carpenter, Santiago Rodriquez Opsina, David J. Merkler *

Department of Chemistry, University of South Florida, Tampa, FL 33620, USA

ARTICLE INFO

Article history:
Received 11 October 2013
Revised 11 December 2013
Accepted 27 December 2013
Available online 18 January 2014

Edited by Judit Ovádi

Keywords:
Arylalkylamine *N*-acyltransferase
Arylalkylamine *N*-acetyltransferase
N-acyldopamine
N-acylserotonin
Thorax-abdomen
Steady-state kinetics
Drosophila melanogaster

ABSTRACT

Arylalkylamine *N*-acyltransferase-like 2[2] (AANATL2) from *Drosophila melanogaster* was expressed and shown to catalyze the formation of long-chain *N*-acylserotonins and *N*-acydopamines. Subsequent identification of endogenous amounts of *N*-acylserotonins and colocalization of these fatty acid amides and *AANATL2* transcripts gives supporting evidence that AANATL2 has a role in the biosynthetic formation of these important cell signalling lipids.

1. Introduction

Fatty acid amides are an emerging class of cell signalling lipids. This family of bioactive amides consists of *N*-acyl amino acids, *N*-acylarylalkylamines, *N*-acylethanolamides, *N*-monoacylpolyamines, and primary fatty acid amides. The *N*-acylarylalkylamides can be subdivided into two groups called the *N*-acyldopamines and the *N*-acylserotonins. With the exception of the *N*-acylethanolamines, the biosynthetic routes to these long-chain fatty acid amides *in vivo* is largely unknown [1,2].

The *N*-acylserotonins were originally synthesized as inhibitors of fatty acid amino hydrolase (FAAH), the primary focus being *N*-arachidonoylserotonin with an IC_{50} = 12 μM [3]. Following this discovery, *N*-arachidonoylserotonin was shown to act as a vanilloid TRPV1 receptor antagonist [4], as an inhibitor of soybean lipoxygenase [5], as a regulator for gastric emptying [6], and also exhibited analgesic, anxiolytic, and anti-allergic activity in various model systems [4,7–8]. The biological roles for the other known long-chain *N*-acylserotonins have yet to be determined. Recently, Verhoeckx et al. [9] identified and quantified the endogenous amounts of long-chain *N*-acylserotonins in the different regions of the porcine gastrointestinal tract, including the ileum. Like the *N*-acylserotonins, activities have been ascribed to the *N*-acyldopamines, as the *N*-acyldopamines regulate pain perception, body temperature, and locomotion in mammals [10–13]. Little is known about the *in vivo* production of the *N*-acylserotonins and *N*-acyldopamines except for data showing that these could be produced by the direct conjugation of serotonin or dopamine to a fatty acid [9,14]. One set of biosynthetic reactions consistent with these data would be the initial formation of the acyl-CoA in a reaction requiring adenosine triphosphate (ATP), followed by a reaction between the resulting acyl-CoA and serotonin or dopamine to form the long-chain *N*-acylarylalkylamide (Fig. 1). Acyl-CoA formation is catalyzed by an acyl-CoA synthetase, a known enzyme [15], while

Abbreviations: AANATL2, arylalkylamine *N*-acyltransferase like 2; FAAH, fatty acid amino hydrolase; ATP, adenosine triphosphate; AANAT, arylalkyamine *N*-acetyltransferase; *D. melanogaster*, *Drosophila melanogaster*; *E. coli*, *Escherichia coli*; SDS–PAGE, sodium dodecyl sulfate polyacrylamide gel electrophoresis; DTNB, 5,5′-dithiobis(2-nitrobenzoic acid); RT-PCR, reverse transcription polymerase chain reaction; LC/QTOF-MS, liquid chromatography/quadrupole time-of-flight mass spectrometry

* Corresponding author. Address: Department of Chemistry, 4202 E. Fowler Ave., CHE 205, Tampa, FL 33620-5250, USA. Fax: +1 813 974 3203.

E-mail address: merkler@usf.edu (D.J. Merkler).

[1] Co-first authorship.

[2] The authors recommend the change of arylalkylamine *N*-acetyltransferase to arylalkylamine *N*-acyltransferase due to the discovery of acyl-CoA substrates longer than C2 (acetyl).

http://dx.doi.org/10.1016/j.febslet.2013.12.027

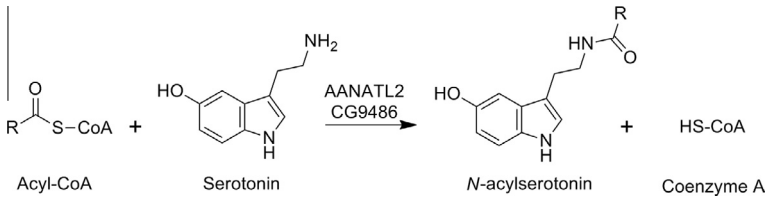

Fig. 1. Proposed reaction for the formation of long-chain *N*-acylserotonins catalyzed by AANATL2.

the enzyme catalyzing the second reaction is reported here for the first time. This chemistry is consistent with reactions catalyzed by the arylalkylamine *N*-acetyltransferases (AANATs) and other enzymes of the GCN5-related *N*-acetyltransferase (GNAT) family enzymes [16–18].

AANATs from a number of organisms have been shown to catalyze the production of different *N*-acetylarylalkylamides like *N*-acetyldopamine and *N*-acetylserotonin [16–18]. Other than a single report that propionyl-CoA and butyryl-CoA are relatively poor substrates for human serotonin *N*-acetyltransferase [19], it has not been determined if the known AANATs will utilize long-chain acyl-CoA thioesters as substrates to generate the corresponding long chain *N*-acylarylalkylamides [19]. Eight putative arylalkylamine *N*-acetyltransferase-like (AANATL) enzymes [20] were identified in *Drosophila melanogaster* and we hypothesized that one of these enzymes would have a role in the formation of the long-chain *N*-acylserotonins.

Herein, we provide evidence that arylalkylamine *N*-acyltransferase like 2 (AANATL2), an AANATL enzyme from *Drosophila melanogaster* (*D. melanogaster*) (CG9486), will catalyze the formation of long-chain *N*-acylserotonins. We further define the expression of AANATL2 transcripts in different anatomical regions of the flies and find measureable levels of the endogenous *N*-acylserotonins in regions that overlap with the expression of the AANATL2 transcripts. While the *N*-acylserotonins are the major focus of this report, we also demonstrate that arylalkylamines other than serotonin are AANATL2 substrates, including dopamine, octopamine, and tyramine. These data suggest that AANATL2 could serve broadly in the cellular production of numerous different *N*-acylarylalkylamides.

2. Materials and methods

2.1. Materials

Codon optimized *AANATL2* was purchased from Genscript. Oligonucleotides were purchased from Eurofins MWG Operon. BL21(DE3) *Escherichia coli* competent cells and *pET-28a*(+) vector were purchased from Novagen. Probond™ nickel-chelating resin, Ambion MicroPoly(A) Purist, and Ambion Retroscript kit were purchased from Invitrogen. *NdeI*, *XhoI*, Antarctic Phosphatase, and T4 DNA ligase were purchased from New England Biolabs. Ampicillin sodium salt and IPTG were purchased from Gold Biotechnology. Long-chain acyl-CoAs were purchased from Sigma–Aldrich. *D. melanogaster* (Oregon R) and 4–24 Instant Medium were supplied by Carolina Biological. Silica was purchased from Suppelco. Long-chain *N*-acylserotonins and *N*-arachidonoylglycine-d_8 standards were purchased from Cayman Chemical. All other reagents were of the highest quality available from either Sigma–Aldrich or Fisher Scientific.

2.2. Molecular cloning

2.2.1. AANATL2

(CG9486; Accession No. NM_135161.3) was codon optimized for expression in *Escherichia coli* (*E. coli*) and purchased from Genscript. The codon optimized gene was inserted into a *pET28a*(+) vector using the *NdeI* and *XhoI* restriction sites. The *AANATL2-pET28a* vector was then transformed into *E. coli* BL21(DE3) competent cells and plated on a LB agar plate supplemented with 40 μg/mL kanamycin. A single colony from the transformation was then used for the expression of AANATL2.

2.3. Protein expression and purification

The BL21(DE3) *E. coli* cells containing the *D. melanogaster AANATL2-pET28a* vector were cultured in LB media supplemented with 40 μg/mL kanamycin and induced with 1 mM isopropyl β-D-1-thiogalactopyranoside at an OD_{600} of 0.6 for 4 h at 37 °C. The final culture was then harvested by centrifugation at 5000*g* for 10 min at 4 °C and the pellet was collected.

The pellet was then resuspended in 20 mM Tris, 500 mM NaCl, 5 mM imidazole; lysed by sonication; and then centrifuged at 10000*g* for 15 min at 4 °C. The resulting supernatant was loaded onto 6 mL of Probond™ nickel-chelating resin. The column was first washed with 10 column volumes of 20 mM Tris–HCl, 500 mM NaCl, 5 mM imidazole, pH 7.9, then washed with 10 column volumes of 20 mM Tris–HCl, 500 mM NaCl, 60 mM imidazole, pH 7.9, and lastly eluted in 1 mL fractions of 20 mM Tris–HCl, 500 mM NaCl, 500 mM imidazole, pH 7.9. The AANATL2 within these fractions were analyzed for purity using a 10% sodium dodecyl sulfate polyacrylamide gel electrophoresis (SDS–PAGE) gel, visualized using Coomassie stain, and pooled together. The pooled fractions are dialyzed overnight at 4 °C in 20 mM Tris, 200 mM NaCl, pH 7.4 and stored at −80 °C.

2.4. Activity assay

Steady-state kinetic characterization of AANATL2 was performed in 300 mM Tris–HCl, pH 8.0, 150 μM 5,5′-dithiobis(2-nitrobenzoic acid) (DTNB) [21], and varying concentrations of substrates. Initial rates were measured continuously at 412 nm. Kinetic constants for long-chain acyl-CoA substrates were determined by holding the initial serotonin concentration constant at 5 mM. Kinetic constants for the short-chain acyl-CoA substrates, acetyl-CoA and butyryl-CoA, were determined by holding the initial serotonin concentration constant at 100 μM. The steady-state kinetic constants for serotonin, dopamine, octopamine, and tyramine were delineated by holding the initial acyl-CoA concentration at 50 μM. Steady-state kinetic constants were obtained by fitting the data to the Michaelis–Menten equation in SigmaPlot 12.0.

2.5. AANATL2 product characterization

The product of the AANATL2-catalyzed reaction was generated by incubating 36 μg of the enzyme for 1 h in 300 mM Tris–HCl, pH 8.0, 50 mM serotonin or dopamine, and 500 μM oleoyl-CoA. The reaction mixture was passed through a 10 kDa ultrafilter (Millipore) to remove the AANATL2 and resulting protein-free solution injected on an Agilent 6540 liquid chromatography/quadrupole time-of-flight mass spectrometer (LC/QTOF-MS) in positive ion mode. A Kinetex™ 2.6 μm C18 100 Å (50 × 2.1 mm) reverse phase

column was used for AANATL2 product separation. Mobile phase A consisted of water with 0.1% formic acid and mobile phase B consisted of acetonitrile with 0.1% formic acid. A linear gradient of 10% B increasing to 100% B over the course of 5 min, followed by a hold of 3 min at 100% B was used for the LC analysis of the reaction product. The reverse phase column was equilibrated with 10% B for 8 min after the run to prepare the column for the subsequent injections.

2.6. AANATL2 transcript localization

D. melanogaster were grown on 4–24 Instant Medium from Carolina Biological, flash frozen for decapitation, and the heads were separated from thorax-abdomens using a wired mesh. Ambion MicroPoly(A) Purist kit was used to purify the mRNA and Ambion Retroscript kit was used to generate the cDNA library for subsequent reverse transcription polymerase chain reaction (RT-PCR) localization of *AANATL2* from *D. melanogaster* head and thorax-abdomen. Identification of *AANATL2* transcripts was completed by RT-PCR (45 cycles of 95 °C for 30 s; 60 °C for 30 s; 72 °C for 1 min). The primers used to amplify a 247 bp region of *AANATL2* (forward – ATGACAATCGGGGATTACGA, reverse – CCTCCTGGTACTCCCTCTCC) were designed and synthesized by Eurofins MWG Operon. Amplified product from the RT-PCR reaction was analyzed by a 0.6% agarose gel and the band visualized by 0.5 μg/mL ethidium bromide under ultraviolet light. The positive bands at 247 bp were cut out of the gel, purified by the Promega Wizard® SV Gel and PCR Clean-up system, and sequenced by Eurofins MWG Operon.

2.7. Endogenous quantification of long-chain N-acylserotonins

Four separate cultures of *D. melanogaster* were used for the analysis of endogenous levels of long-chain *N*-acylserotonins. Lipids were extracted using organic solvents followed by the solid phase purification of Farrell et al. [22]. The purified extracts were dried under N_2, reconstituted in HPLC grade methanol, and injected on an Agilent 1260 connected to an Agilent 6540 LC/QTOF-MS in positive ion mode. Injected lipid extracts were separated by a Kinetex™ 2.6 μm C_{18} 100 Å (50 × 2.1 mm) reverse phase column at 0.6 mL/min. Mobile phase A consisted of water with 0.1% formic acid and mobile phase B consisted of acetonitrile with 0.1% formic acid. A linear gradient was used for the separation of the injected lipid extracts by reverse phase chromatography starting at 10% B and increasing to 100% B over the course of 5 min, followed by a hold of 3 min at 100% B. The reverse phase column was equilibrated with 10% B for 8 min after the run to prepare the column for subsequent injections. *N*-Arachidonoylglycine-d_8, 1 pmol per 10 μL injection, was spiked into each extraction to measure instrument performance and for data normalization. The four extractions from separate cultures of *D. melanogaster* were analyzed in triplicate for a total of 12 runs. Standard curves of commercially available *N*-acylserotonins and *N*-arachidonoylglycine-d_8 were analyzed in triplicate with a linear range of 100 fmoles to 5 pmol (r^2 values >0.99).

3. Results and discussion

The codon optimized *D. melanogaster AANATL2* gene was prepared commercially by Genscript and cloned into a *pet28a*(+) vector that encodes for an N-terminal His_6-tag protein. Recombinant *D. melanogaster* AANATL2 was expressed in *E. coli* BL21(DE3) cells and purified using Probond™ nickel-chelating resin. The purified AANATL2 was then analyzed by SDS–PAGE (Fig. 2), yielding a single band at 25 kDa.

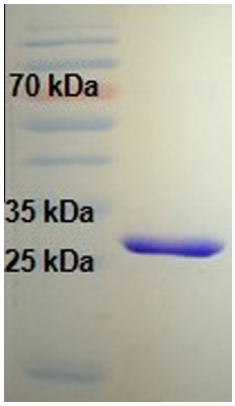

Fig. 2. SDS-PAGE analysis of purified *D. melanogaster* AANATL2. Left lane is PageRuler™ Prestained Protein Ladder. Right lane is purified AANATL2.

Potential substrates for AANATL2 were identified using Ellman's reagent [21] by measuring the acyl-CoA dependent release of CoA-SH which yields 2-nitro-5-thiobenzoate at 412 nm. Activity was observed with serotonin and oleoyl-CoA from our substrate screening studies which was evaluated in greater detail with subsequent steady-state kinetic analysis of AANATL2 with a set of acyl-CoA thioesters and serotonin. We found that acyl-CoA thioesters from acetyl-CoA to arachidonoyl-CoA are AANATL2 substrates with some variability in the apparent kinetic constants at saturating serotonin. The $(K_{M,acyl\text{-}CoA})_{app}$ values for all the acyl-CoA thioesters included in our study were approximately the same, ranging from ~2 μM for butyryl-CoA and arachidonoyl-CoA to ~10 μM for palmitoyl-CoA. Greater variability was observed for the $(k_{cat,acyl\text{-}CoA})_{app}$ and $(k_{cat}/K_M)_{acyl\text{-}CoA,app}$ values with a range of 20–30-fold. Based on our data, the short-chain acyl-CoA thioesters are, in general, substrates with higher $(k_{cat}/K_{M,acyl\text{-}CoA})_{app}$ values than the long-chain acyl-CoA thioesters (Table 1). Amherd et al. [20] expressed *D. melanogaster* AANATL2 in COS-7 cells and report a $(K_{M,acyl\text{-}CoA})_{app}$ for acetyl-CoA of 7.2 ± 0.6 μM with tryptamine as a co-substrate that is similar to the value we measure using serotonin as the co-substrate. A comparison of $(k_{cat,acyl\text{-}CoA})_{app}$ and $(k_{cat}/K_M)_{acyl\text{-}CoA,app}$ values we measure (Table 1) to those reported by Amherd et al. [20] is difficult as these researchers did not purify recombinant AANATL2 from the COS-7 cells.

We have also evaluated biologically relevant arylalkylamines other than serotonin as substrates for AANATL2, namely dopamine, octopamine, and tyramine. Ahmerd et al. [20] have already demonstrated that tryptamine is a substrate for *D. melanogaster* AANATL2. Neither tyramine nor octopamine were substrates when the acyl acceptor was oleoyl-CoA as the observed rate of CoA release from oleoyl-CoA was equivalent to the background rate of hydrolysis

Table 1
Acyl-CoA specificity for AANATL2.

Substrate[a]	$(K_{M,acyl\text{-}CoA})_{app}$ μM	$(k_{cat,acyl\text{-}CoA})_{app}$ s^{-1}	$(k_{cat}/K_M)_{acyl\text{-}CoA,app}$ $M^{-1}\,s^{-1}$
Acetyl-CoA	6.1 ± 0.27	1.3 ± 0.012	(2.2 ± 0.020) × 10^5
Butyryl-CoA	1.8 ± 0.17	0.53 ± 0.011	(2.9 ± 0.058) × 10^5
Palmitoyl-CoA	9.9 ± 1.6	0.16 ± 0.0090	(1.6 ± 0.091) × 10^4
Stearoyl-CoA	6.0 ± 0.75	0.059 ± 0.0023	(9.8 ± 0.39) × 10^3
Oleoyl-CoA	3.6 ± 0.58	0.075 ± 0.0033	(2.1 ± 0.091) × 10^4
Arachidonoyl-CoA	1.9 ± 0.25	0.043 ± 0.0013	(2.3 ± 0.068) × 10^4

[a] Background rates of acyl-CoA hydrolysis were obtained at each CoA concentration in the absence of serotonin and subtracted from the rate obtained in the presence of serotonin. The non-serotonin background rates were ⩽15% of rates obtained in the presence of serotonin, with exception of steroyl-CoA. For stearoyl-CoA, the background hydrolysis rates were ⩽30%.

obtained in the absence of the arylalkylamine. However, both were substrates when the acyl acceptor was acetyl-CoA. The kinetic constants for the AANATL2-catalyzed formation of *N*-acetyltyramine and *N*-acetyloctopamine are similar to those determined for the formation of *N*-acetylserotonin except for a relatively high $(K_{M,amine})_{app}$ for octopamine of 78 ± 3.9 μM (Table S1, Supplementary Materials). Dopamine is a substrate for AANATL2 when the co-substrate is acetyl-, palmitoyl-, or oleoyl-CoA (Table 2). Again, the kinetic constants for the formation of *N*-acetyldopamine are similar to those determined for the generation of the other *N*-acetylarylalkylamides.

We evaluated the relationship between the $(K_{M,amine})_{app}$ for serotonin or dopamine as a function of acyl chain length for the acyl-CoA substrates (Table 2) because both of these were substrates when acetyl-CoA and the long-chain acyl-CoA were co-substrates. The pattern in the data was the same for both serotonin and dopamine, the $(K_{M,amine})_{app}$ increased, the $(k_{cat,amine})_{app}$ decreased, and the $(k_{cat}/K_M)_{amine,app}$ decreased as the acyl chain length increased from acetyl to arachidonoyl. The ratio of $(k_{cat}/K_M)^{acetyl-CoA}_{amine,app}/(k_{cat}/K_M)^{arachidonoyl-CoA}_{amine,app}$ is 3400 for dopamine and 5000 for serotonin indicating that acetyl-CoA is substantially preferred by AANATL2. Side-by-side comparisons of the acyl-CoA thioesters between serotonin and dopamine show that AANATL2 exhibits a slight preference for serotonin as the amine donor substrate.

An examination of our kinetic data reveals some patterns: (a) limited variation in the $(K_{M,acyl\text{-}CoA})_{app}$ values for the acyl-CoA substrates as all are in the range of 2–10 μM, (b) limited variation $(k_{cat,amine})_{app}$ and $(k_{cat}/K_M)_{amine,app}$ values on the amine substrate, (c) an increase in the $(K_{M,amine})_{app}$ values for the amine substrates as the length of the acyl chain increases for the acyl-CoAs, and (d) a decrease in the $(k_{cat,amine})_{app}$ and $(k_{cat}/K_M)_{amine,app}$ values as the length of the acyl chain increases for the acyl-CoAs. These data suggest that the long-chain acyl group either interferes with the binding of the arylalkylamine substrates or that the binding of the long-chain acyl-CoAs results in an AANATL2 conformation that is less optimal for catalysis. An X-ray structure of AANATL2 with bound acetyl-CoA or oleoyl-CoA could differentiate between these two possibilities. We also note the relatively low $k_{cat,app}$ values [$(k_{cat,acyl\text{-}CoA})_{app}$ and $(k_{cat,amine})_{app}$] values for the long-chain acyl-CoA substrates; however, low $k_{cat,app}$ values are not surprising since the long-chain *N*-acyl-serotonins and dopamines likely serve as potent cell signaling lipids [9–13]. The cellular function of AANATL2 may be the generation of the long-chain *N*-acylarylalkylamides and the measured $k_{cat,app}$ values are sufficient to supply the cellular needs of these potent lipid amides. Saghatelian and Cravatt [23] have shown in their studies of FAAH(−/−) that *in vitro* measurements of kinetic constants may not provide a complete understanding of the functional role of an enzyme *in vivo*.

Table 2
Apparent kinetic constants for serotonin and dopamine using different acyl-CoA substrates.

Substrate[a]	$(K_{M,amine})_{app}$ μM	$(k_{cat,amine})_{app}$ s^{-1}	$(k_{cat}/K_M)_{amine,app}$ $M^{-1}\,s^{-1}$
Serotonin			
Acetyl-CoA	7.2 ± 1.1	2.4 ± 0.097	$(3.3 \pm 0.13) \times 10^5$
Butyryl-CoA	2.9 ± 0.33	0.52 ± 0.011	$(1.8 \pm 0.040) \times 10^5$
Palmitoyl-CoA	870 ± 60	0.15 ± 0.0034	$(1.7 \pm 0.039) \times 10^2$
Stearoyl-CoA	350 ± 35	0.057 ± 0.0014	$(1.6 \pm 0.040) \times 10^2$
Oleoyl-CoA	490 ± 86	0.085 ± 0.0059	$(1.7 \pm 0.12) \times 10^2$
Arachidonoyl-CoA	460 ± 69	0.030 ± 0.0014	66 ± 3.0
Dopamine			
Acetyl-CoA	0.042 ± 0.0097	6.5 ± 0.67	$(1.6 \pm 0.16) \times 10^5$
Palmitoyl-CoA	1.1 ± 0.13	0.14 ± 0.0050	$(1.2 \pm 0.045) \times 10^2$
Oleoyl-CoA	1.2 ± 0.20	0.058 ± 0.0033	47 ± 2.7

[a] Background rates of acyl-CoA hydrolysis were obtained at a saturating CoA concentration in the absence of the arylalkylamine and subtracted from the rate obtained in the presence of arylalkylamine. The non-arylalkylamine (background rates) were ⩽20% of rates obtained in the presence of arylalkylamine.

Table 3
Standards used for identification of endogenous long-chain *N*-acylserotonins and the AANATL2 product characterization.

N-acylarylalkylamide standard	Retention time min	Molecular ion $[M+H]^+$ *m/z*
N-oleoylserotonin	6.132	441.3878
N-palmitoylserotonin	6.038	415.3344
N-stearoylserotonin	6.368	443.3620
N-arachidonoylserotonin	5.900	463.3291
N-oleoyldopamine	5.929	418.3326
AANATL2 product[a]	6.130	441.3464
AANATL2 product[b]	5.929	418.3325

[a] Reaction conditions: 300 mM Tris–HCl, pH 8.0, 50 mM serotonin, and 500 μM oleoyl-CoA was incubated with 36 μg of AANATL2 for 1 h.
[b] Reaction conditions: 300 mM Tris–HCl, pH 8.0, 50 mM dopamine, and 500 μM oleoyl-CoA was incubated with 36 μg of AANATL2 for 1 h.

The products from the AANATL2 catalyzed reaction between oleoyl-CoA and serotonin or dopamine were positively identified as *N*-oleoylserotonin and *N*-oleoyldopamine (Table 3). AANATL2 was incubated with serotonin or dopamine and oleoyl-CoA for 1 h, the enzyme was removed by ultrafiltration using a 10 kDa cut-off filter, followed by product analysis by liquid chromatography/quadrupole time-of-flight mass spectrometry (LC/QTOF-MS). AANATL2-generated *N*-oleoylserotonin or *N*-oleoyldopamine was compared to a commercial standard. Positive identification was delineated by a comparable retention time and molecular ion *m/z* for the AANATL2 product and the standard (Table 3).

The *in vitro* data we obtained using purified AANATL2 (substrate specificity and product characterization) lead to questions such as: (a) are the long-chain *N*-acylarylalkylamides found in *D. melanogaster*, (b) if so, what are the steady-state endogenous levels of these fatty acid amides, and (c) would we find colocalization of endogenous *N*-acylarylalkylamides and AANATL2? To address these intriguing questions, we first identified the localization of the AANATL2 transcripts by RT-PCR. Primers were designed and synthesized commercially to generate a 247 bp *AANATL2*-derived RT-PCR product from the cDNA libraries generated from *D. melanogaster* head and thorax-abdomen. The RT-PCR experiments show that *AANATL2* transcripts were only found in the thorax-abdomen of *D. melanogaster* (Fig. 3).

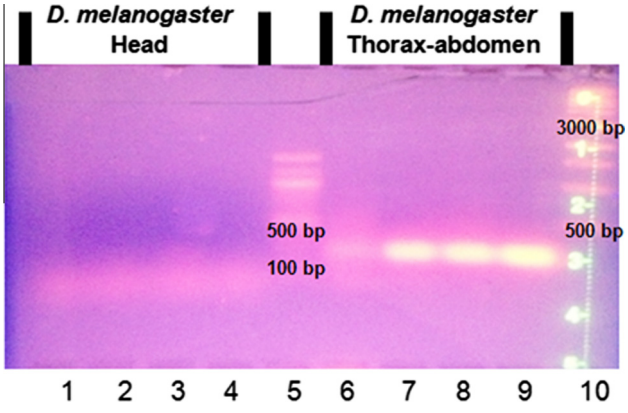

Fig. 3. RT-PCR of AANATL2 in *D. melanogaster* head and thorax-abdomen. Lanes 1–4 is data generated from the *D. melanogaster* head cDNA library at 45, 50, 55, and 60 °C annealing temperatures respectively. Lane 5 is 100 bp DNA ladder from New England Biolabs. Lanes 6–9 is data generated from the *D. melanogaster* thorax-abdomen cDNA library at 45, 50, 55, and 60 °C annealing temperature respectively. Lane 10 is a 1 kb DNA ladder from New England Biolabs.

Table 4
Endogenous amounts of *N*-acylserotonins found in *D. melanogaster* head and thorax-abdomen.

N-acylserotonin	Head[a]	Thorax-abdomen[b]		
	Extracted amount pmoles g^{-1}	Extracted amount pmoles g^{-1}	Retention time min	Molecular ion $[M+H]^+$ m/z
N-oleoylserotonin	nd[c]	0.42 ± 0.55	6.147	441.2633
			6.009	441.2684
			6.149	441.2666
			6.180	441.2622
N-palmitoylserotonin	nd[c]	1.16 ± 0.12	6.036	415.3249
			6.032	415.3237
			6.040	415.3243
N-stearoylserotonin	nd[c]	53.5 ± 33.3	6.367	443.3143
			6.244	443.2986
			6.368	443.3167
			6.262	443.2993
N-arachidonoylserotonin	nd[c]	0.25 ± 0.15	5.907	463.2998
			5.906	463.3022
			5.882	463.3478
			5.940	463.3138

[a] Identification and quantification of endogenous amounts extracted from 1 g of *D. melanogaster* heads.
[b] Identification and quantification of endogenous amounts extracted from 1 g of *D. melanogaster* thorax-abdomen.
[c] nd indicates that these *N*-acylserotonins were "not detected" in 1 g of this anatomical location of *D. melanogaster*.

AANATL2 was positively identified by the 247 bp RT-PCR product generated from the *D. melangaster* thorax-abdomen cDNA library; however, a similar RT-PCR product was not observed from the head cDNA library. The sequence of the 247 bp product from the thorax-abdomen library was confirmed as *AANATL2* by DNA sequencing. These data are in slight contrast to the report a faint band for *AANATL2* from *D. melanogaster* head by Northern analysis [20]. Together, our data and that from Amherd et al. [20] indicate that *AANATL2* transcripts are found at substantially higher levels in the thorax-abdomen relative to the head in *D. melanogaster*.

Our identification of the *AANATL2* transcripts in the thorax-abdomen and the relatively high levels of serotonin in the mammalian gastrointestinal tract [9,24] strongly suggested to us that the long-chain *N*-acylserotonins would exist endogenously in the thorax-abdomen of *D. melanogaster*. Four long-chain *N*-acylserotonins were identified in the thorax-abdomen by molecular ion m/z and retention time comparisons to commercially available standards (Table 4) by LC/QTOF-MS in positive ion mode. Endogenous amounts of *N*-acylserotonins were not identified in the heads, consistent with our RT-PCR data in which the *AANATL2* transcripts were not found. Standard curves with a linear range of 100 fmoles to 5 pmol (r^2 values >0.99) were used to quantify the endogenous amounts of *N*-acylserotonins in the thorax-abdomen. *N*-Stearoylserotonin was the most abundant followed by *N*-palmitoylserotonin, *N*-arachidonoylserotonin, and *N*-oleoylserotonin (Table 4). The *N*-acylserotonin levels that we found in the thorax-abdomen of *D. melanogaster* are similar to that reported for these fatty acid amides in porcine gastrointestinal tract [9]. In contrast to the long-chain *N*-acylserotonins, the long-chain *N*-acyldopamines are found in both the thorax-abdomen and the heads of *D. melanogaster* [25]. The dissimilarities in the localization of the long-chain *N*-acylserotonins relative to the long-chain *N*-acyldopamines are likely the result of differences in biosynthesis, degradation, and/or transport of these different *N*-acylarylalkylamides.

In summary, AANATL2 from *D. melanogaster* was shown to catalyze the formation of a diverse set of *N*-acylarylalkylamides with the most intriguing products being the long-chain *N*-acylserotonins and *N*-acyldopamines. Colocalization of *AANATL2* transcripts and endogenous long-chain *N*-acylserotonins to the thorax-abdomen points to an important role for this enzyme in the biosynthesis of these cell signalling long-chain *N*-acylarylalkylamides. Future work to expand our understanding of biosynthesis and degradation of the *N*-acylserotonins, *N*-acyldopamines, and other long-chain *N*-acylarylalkylamides involving the inhibition of key enzymes is ongoing.

Acknowledgments

This work has been support, in part, by Grants from the National Institutes of Health (R03-DA034323) and the Florida Center for Excellence for Biomolecular Identification and Targeted Therapeutics (FCoE-BITT Grant No. GALS020) and support from the Mass Spectrometry and Peptide Facility, Department of Chemistry, University of South Florida. The authors acknowledge Dr. Ryan Young for many helpful discussions and Dr. K. Kenneth Caswell for a critical reading of the manuscript.

Appendix A. Supplementary data

Supplementary data associated with this article can be found, in the online version, at http://dx.doi.org/10.1016/j.febslet.2013.12.027.

References

[1] Farrell, E.K. and Merkler, D.J. (2008) Biosynthesis, degradation and pharmacological importance of the fatty acid amides. Drug Discov. Today 13, 558–568.
[2] Okamoto, Y., Tsuboi, K. and Ueda, N. (2009) Enzymatic formation of anandamide. Vitam. Horm. 81, 1–24.
[3] Bisogno, T. et al. (1998) Arachidonoylserotonin and other novel inhibitors of fatty acid amide hydrolase. Biochem. Biophys. Res. Commun. 248, 515–522.
[4] Maione, S. et al. (2007) Analgesic actions of N-arachidonoyl-serotonin, a fatty acid amide hydrolase inhibitor with antagonistic activity at vanilloid TRPV1 receptors. Br. J. Pharmacol. 150, 766–781.
[5] Nguyen, M.D., Nguyen, D.H., Yoo, J.M., Myung, P.K., Kim, M.R. and Sok, D.E. (2013) Effect of endocannabinoids on soybean lipoxygenase-1 activity. Bioorg. Chem. 49, 24–32.
[6] Di Marzo, V. et al. (2008) The role of endocannabinoids in the regulation of gastric emptying: alterations in mice fed a high-fat diet. Br. J. Pharmacol. 153, 1272–1280.
[7] Yoo, J.M., Sok, D.E. and Kim, M.R. (2013) Effect of endocannabinoids on IgE-mediated allergic response in RBL-2H3 cells. Int. Immunopharmacol. 17, 123–131.
[8] Micale, V., Cristino, L., Tamburella, A., Petrosino, S., Leggio, G.M., Drago, F. and Di Marzo, V. (2009) Anxiolytic effects in mice of a dual blocker of fatty acid amide hydrolase and transient receptor potential vanilloid type-1 channels. Neuropsychopharmacology 34, 593–606.

[9] Verhoeckx, K.C.M., Voortman, T., Balvers, M.G.J., Hendriks, H.F.J., Wortelboer, H.M. and Witkamp, R.F. (2011) Presence, formation and putative biological activities of N-acyl serotonins, a novel class of fatty-acid derived mediators, in the intestinal tract. Biochim. Biophys. Acta 1811, 578–586.
[10] Bisogno, T., Melck, D., Bobrov, M.Yu., Gretskaya, N.M., Bezuglov, V.V., De Petrocellis, L. and Di Marzo, V. (2000) N-acyl-dopamines: novel synthetic CB(1) cannabinoid-receptor ligands and inhibitors of anandamide inactivation with cannabimimetic activity *in vitro* and *in vivo*. Biochem. J. 351 (Pt 3), 817–824.
[11] Huang, S.M. et al. (2002) An endogenous capsaicin-like substance with high potency at recombinant and native vanilloid VR1 receptors. Proc. Natl. Acad. Sci. USA 99, 8400–8405.
[12] Chu, C.J. et al. (2003) N-oleoyldopamine, a novel endogenous capsaicin-like lipid that produces hyperalgesia. J. Biol. Chem. 278, 13633–13639.
[13] De Petrocellis, L., Chu, C.J., Moriello, A.S., Kellner, J.C., Walker, J.M. and Di Marzo, V. (2004) Actions of two naturally occurring saturated N-acyldopamines on transient receptor potential vanilloid 1 (TRPV1) channels. Br. J. Pharmacol. 143, 251–256.
[14] Akimov, M.G., Gretskaya, N.M., Shevchenko, K.V., Shevchenko, V.P., Myasoedov, N.F., Bobrov, M.Y. and Bezuglov, V.V. (2003) New aspects of biosynthesis and metabolism of *N*-acyldopamines in rat tissues. Russ. J. Bioorg. Chem. 33, 648–652.
[15] Soupene, E. and Kuypers, F.A. (2008) Mammalian long-chain acyl-CoA synthetases. Exp. Biol. Med. (Maywood) 233, 507–521.
[16] Dyda, F., Klein, D.C. and Hickman, A.B. (2000) GCN5-related N-acetyltransferases: a structural overview. Annu. Rev. Biophys. Biomol. Struct. 29, 81–103.
[17] Vetting, M.W., de Carvalho, L.P., Yu, M., Hegde, S.S., Magnet, S., Roderick, S.L. and Blanchard, J.S. (2005) Structure and functions of the GNAT superfamily of acetyltransferases. Arch. Biochem. Biophys. 433, 212–226.
[18] Zheng, W. and Cole, P.A. (2002) Serotonin *N*-acetyltransferase: mechanism and inhibition. Curr. Med. Chem. 9, 1187–1199.
[19] Ferry, G. et al. (2000) Substrate specificity and inhibition studies of human serotonin *N*-acetyltransferase. J. Biol. Chem. 275, 8794–8805.
[20] Amherd, R., Hintermann, E., Walz, D., Affolter, M. and Meyer, U.A. (2000) Purification, cloning, and characterization of a second arylalkylamine *N*-acetyltransferase from *Drosophila melanogaster*. DNA Cell Biol. 19, 697–705.
[21] Ellman, G.L. (1959) Tissue sulfhydryl groups. Arch. Biochem. Biophys. 82, 70–77.
[22] Farrell, E.K., Chen, Y., Barazanji, M., Jeffries, K.A., Cameroamortegui, F. and Merkler, D.J. (2012) Primary fatty acid amide metabolism: conversion of fatty acids and an ethanolamine in $N_{18}TG_2$ and SCP cells. J. Lipid Res. 53, 247–256.
[23] Saghatelian, A. and Cravatt, B.F. (2005) Discovery metabolite profiling – forgoing functional connections between the proteome and metabolome. Life Sci. 77, 1759–1766.
[24] Gershon, M.D. and Tack, J. (2007) The serotonin signaling system: from basic understanding to drug development for functional GI disorders. Gastroenterology 132, 397–414.
[25] K.A. Jeffries, D.R. Dempsey, A.L. Behari, R.L. Anderson, D.J. Merkler, *Drosophila melanogaster* as a model system to study long-chain fatty acid amide metabolism, FEBS Lett. (2014) (submitted for publication).